

The Structure, Magnetic Properties, and 3D Simulation of Deformation Martensite in Fe₈₆Mn₁₃C Alloy

L.I. Kveglis^{*1}, S.Ya. Misevra²

Siberian Federal University, Krasnoyarsk, Svobodny Av. 79, Russian Federation;

D. East Kazakhstan State Technical University, Ust-Kamenogorsk , Protozanov Street, 69, Kazakhstan

^{*}kveglis@list.ru; ²SMisevra@ektu.kz

Abstract

Fe₈₆Mn₁₃C alloy (Gadfield's steel) possesses unique mechanical, electric and magnetic properties. As the alloy is widely used in mechanical engineering, one of the challenges is to study the structure of bulk samples of the alloy with the purpose to improve its mechanical properties. Thanks to the special modulated structure, the alloy holds unique electric and magnetic properties. Another task is to investigate thin films of Fe₈₆Mn₁₃C as a possible solution to the problems of spintronics. Three-dimensional models are suggested to describe the formation of a deformation martensite structure in Fe₈₆Mn₁₃C alloy in the form of self-assembled clusters. The models are based on pilot studies of the alloy structure and properties. It is shown that combinations of anti-ferromagnetic austenite and ferrimagnetic martensite of deformation create unique electric and magnetic properties of Fe₈₆Mn₁₃C alloy in both bulk and thin-film state.

Keywords

Fe₈₆Mn₁₃C Thin Films; Inhomogeneous Structure; Magnetic and Electrical Properties

Introduction

It is known that mechanical properties of steels have been improved thanks to the emergence of martensite, which can be formed due to heat treatment or the result of mechanical impact as it occurs in Gadfield's steel. It is also well noted that the structure of deformation martensite in austenitic steels significantly differs from martensite resulting from training. The self-hardening effect of Gadfield steel is explained by shock loadings.

Fe₈₆Mn₁₃C alloy (Gadfield's steel) in bulk Sedov V.P. represents an anti-ferromagnetic invar . Under shock loading we observed local magnetization in the samples . The structural features of Gadfield's steel cause coexistence of various types of magnetic

ordering in the same sample. To understand the mechanism underlying the observed effects, we investigated the structure and magnetic properties of bulk samples of Gadfield steel and thin-film samples. Due to their unique electric and magnetic properties and low cost, Fe₈₆Mn₁₃C films are of interest to the rapidly developing science of spintronics, which demands new materials with a set of appropriate parameters.

Experimental Details

As an object of research we chose the alloy known as Gadfield constructional steel of a commercial production. The alloy structure (Mn-11.5-15.0%, Si-0.80-1.00%, Cr-1.00 of %, Ni-1.00 of %, % Cu-1.00, the Fe-rest.) was studied by means of spectral, X-ray spectral fluorescent and chemical analyses. Bulk samples of steelwith 10x10x100 mm in size, were exposed to shock loading in pendular a copra. As a result, the sample subjected to an impact didn't exceed 280 J/cm² to the extenf of which it was completely collapsed. At impact strengths of 300-320 J/cm², the sample bent but didn't collapse, and it was completely destroyed having been exposed to the same loading for several minutes.

The surface structure of bulk samples was investigated by means of a scanning electron microscope of JSM – 6390VL.

Fe₈₆Mn₁₃C films were obtained from thermal vacuum evaporation on a VUP-4 installation at a pressure of 10-5 mm Hg upon glass and NaCl substrates. The thin-film samples then underwent cryomachining, i.e. repeated immersion in liquid nitrogen with intermediate endurance at room temperature for several minutes. Since thermal expansion coefficients of the film and the substrate differed several times

from glass or NaCl, the film sample was tested under an effective loading of about 3-4 GPa.

The structure of the films was investigated by the method of translucent electronic microscopy and microdiffraction using PREM- 200 and JEM - 2100 flowmeters.

To study the magnetic properties of bulk and film samples, the method of torques on the magnetometer in fields up to 17kOe was used. The torque dependence of $L = B \times H \times \sin\theta$ (where θ is the angle of rotation of the external magnetic field relative to the sample) has been investigated for steel plates with the size 10mm x 5mm x 0.1mm.

Results and Discussion

In fig. 1 a surface image microslice is provided in a scanning electron microscopy of a bulk Fe86Mn13C sample after shock loading. Separate grains of austenite with lines of shift deformation in the form of dark strips paralleling to each other are visible, and the strips in one grain are connected with the strips in the other grain. The pictures of x-ray diffraction testify to emergence of a new phase – deformation martensite. We have previously demonstrated that this phase was localized in strips of shift deformation of austenite grains. The method of torques showed existence of a non-uniform magnetic structure in such samples. In fig. 2 the torque dependence is given in the magnetic field $H=8$ kOe. Analysis of the torque curves shows that the magnetic structure of the alloy is non-uniform. The alloy possesses magnetic viscosity, i.e. the speed of magnetization depends on time; which is proved by discrepancy of hysteresis sites at various angles of rotation. The angular width of the first site makes $50 \div 120^\circ$, which is 70° , and the angular width of the second site is $260 \div 290^\circ$, which is just 30° .

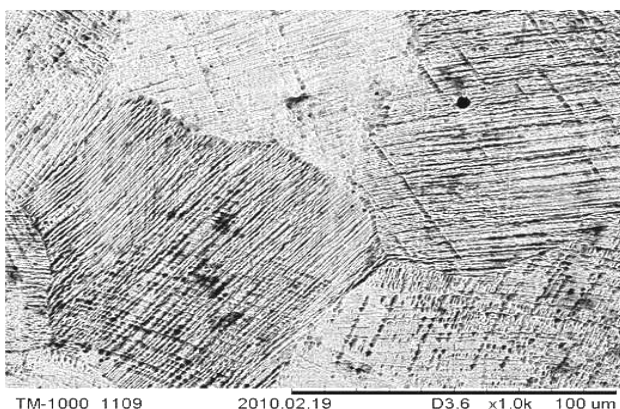


FIG. 1 A SURFACE IMAGE OF THE DEFORMED FE86Mn13C BULK SAMPLE IN A SCANNING ELECTRON MICROSCOPE

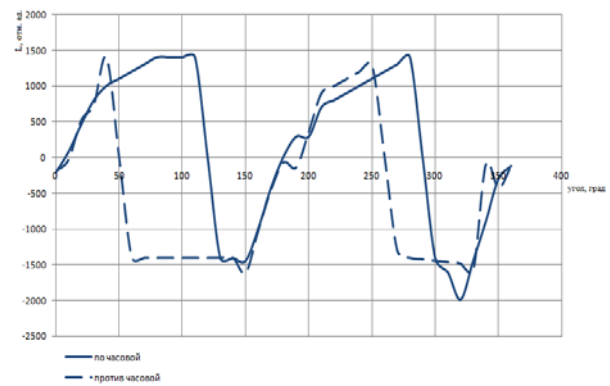


FIG. 2 TORQUE CURVES OF THE DEFORMED FE86Mn13C SPECIMEN ILLUSTRATING HETEROGENEITY OF THE MAGNETIC STRUCTURE

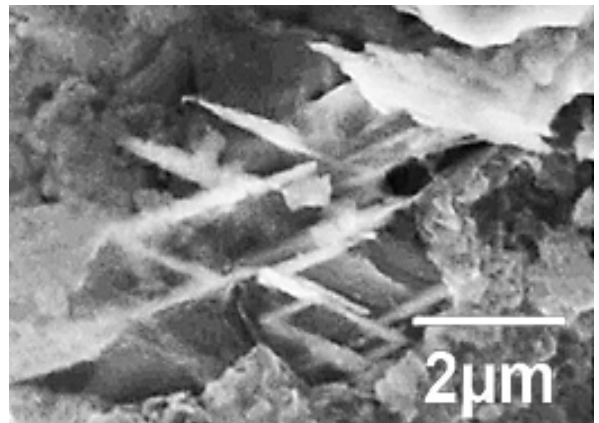


FIG. 3 SECTION MICROGRAPH OF THE FRACTURE SURFACE OF THE FE86Mn13C SAMPLE IN A SCANNING ELECTRON MICROSCOPE JSM 6390 LV.

In Fig. 3 it can be seen that a micrograph of the fracture surface area of the Fe86Mn13C sample is subjected to impact loading pendulum. In the cavity of the fracture crater, a developing phase of deformation martensite has been detected in the form of long needles located at a fixed angle and protruding from the main matrix. The length of the needles is more than that of the main matrix. These needles can only be observed in samples subjected to impact loading .

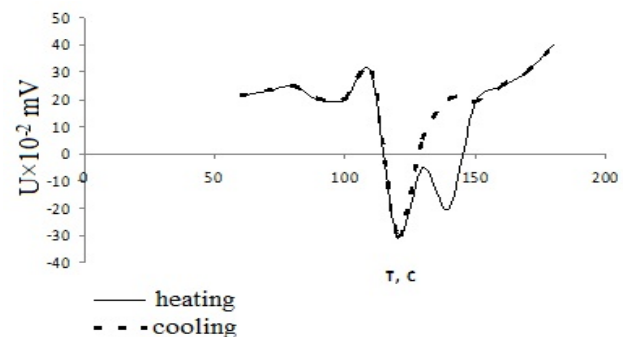


FIG. 4 DEPENDENCE OF THE THERMOELECTRIC POWER ON HEATING AND COOLING OF THE FE86Mn13C SAMPLE

In our earlier papers the dependence of the thermoelectric effect on temperature was discussed.

The voltage dependence on temperature (Fig. 4) shows that it may change sign with temperature. No magnetic field was applied to the sample and yet, the thermoelectric effect reversed its sign at a certain temperature when the sample was heated or cooled.

Fig. 5 shows the ratio R/R_0 , where R is the resistance of the sample at the measurement temperature, and R_0 is the sample resistance at room temperature. It can be seen that the resistance of the original sample (solid line) does not depend on temperature; which is characteristic of invar. The dashed line represents a strained state of the alloy. There is a strong inverse relationship between resistance and temperature; which implies that the alloy behaves like a semiconductor. This behavior is qualitatively consistent with our results, where the spin-polarized calculation assumes a semiconducting state of martensite deformation.

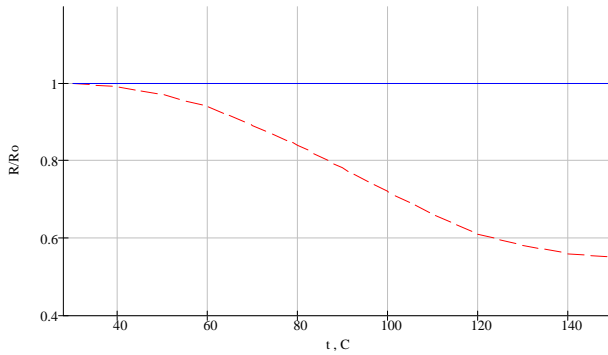


FIG. 5 TEMPERATURE DEPENDENCE OF THE RELATIVE RESISTANCE FOR THE SOURCE (SOLID LINE) AND DEFORMED (DASHED LINE) FE86MN13C.

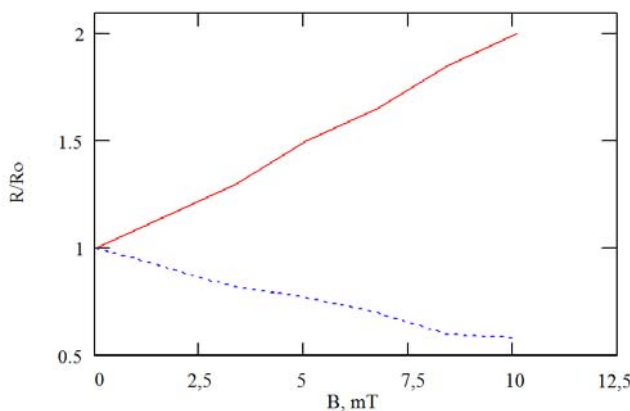


FIG. 6 DEPENDENCE OF MAGNETORESISTANCE ON THE MAGNETIC FIELD OF THE STRAINED FE86MN13C SAMPLE: THE STARTING POSITION OF THE SAMPLE (SOLID LINE), THE SAMPLE IS ROTATED BY 180 DEGREES (DOTTED LINE)

An anomalous behavior of magnetoresistance has been observed in a magnetic field (resistivity in a magnetic field). Figure 6 shows the relative transverse magnetoresistance R/R_0 of the magnetic field H . Here

R is the resistance of the sample under applied field, and R_0 is the resistance of the sample without applied field. Negative magnetoresistance has also been observed when the sample was rotated in the magnetic field $H = 100$ Oe by 180° .

It was found that as a result of machining both samples, bulk and film, exhibited magnetization, which was the evidence of structural and phase transitions under the influence of mechanical loadings. The unique electric and magnetic properties of bulk Fe86Mn13C and the alloy films are due to coexistence of structures of antiferromagnetic austenite and ferrimagnetic martensite of deformation. The samples where the impact strength was not exceeding 280 J/cm² did not show any striate modulated structures and, hence any electric and magnetic properties was excluded from feature.

As the search for new materials for spintronics involves creation of thin-film samples, our further task is to investigate the structure and properties of thin films of Fe86Mn13C alloy.

We studied Fe86Mn13C films characterized with a non-uniform magnetic structure. The heterogeneity is associated with heterogeneity of the crystal structure of the films where austenite with an antiferromagnetic structure coexists with martensite of deformation having a ferrimagnetic order. Martensite of deformation in the films was the result of cryomachining.

In fig. 7 a high-resolution electron microscopy image of a Fe86Mn13C film is shown. coherent coupling of the adjacent clusters can be observed. Each nuclear plane of one cluster passes into the nuclear plane of another cluster. Thus, individual clusters gather in cluster units to form a film.

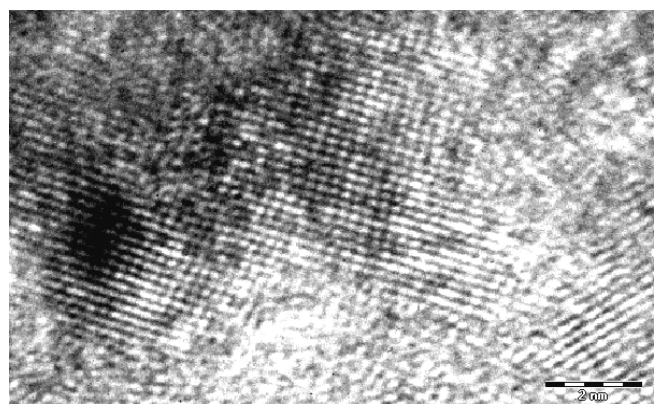


FIG. 7 THE IMAGE OF A CLUSTER STRUCTURE IN THE FE86MN13C FILM OBTAINED BY HIGH-RESOLUTION ELECTRON MICROSCOPY.

There is a dark area visible in the left part of figure 7 . A striate contrast as shown in fig. 8 is formed in the dark area after some seconds of focusing an electron beam onto this area. It is difficult to interpret such contrast as a moire pattern due to the smallness of the size of the area . Besides, the dark color is not caused by the amplitude difference but rather is the resultant phase contrast as the electron beam deviates the magnetic field of the cluster. The dark area was formed as a result of the lack of electrons. Surplus electrons formed the light areas. The striate structure represents a mix of martensite of deformation and austenite, which occurs when the site is heated by an electron beam. Here the magnetic martensite phase remains dark while the austenitic phase brightens.

The magnetic anisotropy implies coherent coupling between separate structural elements of the film. In fig. 9 the torque curves obtained for a Fe86Mn13C film after cryomachining are shown. The given torque curves at the external magnetic field $H=8\text{kOe}$ show that the film magnetization has a pronounced anisotropy and an anisotropic hysteresis. The anisotropy can be associated with the needle form of alternating phases of martensite of deformation and austenite. In our samples, the needle form of martensite of deformation appears both in bulk and film samples.

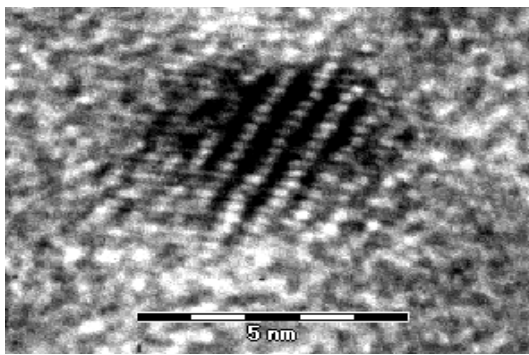


FIG. 8 THE IMAGE IN A HIGH-RESOLUTION TRANSMISSION ELECTRON MICROSCOPE OF THE MAGNETIC CLUSTER FILM FE86MN13C SUBJECTED TO CRYOMECHANICAL PROCESSING IN LIQUID NITROGEN.

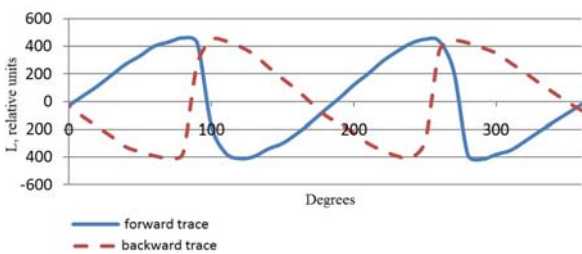


FIG. 9. TORQUE CURVES $L = B \times H \times \sin\theta$ OF THE FE86MN13C FILM AFTER TO CRYOMECHANICAL PROCESSING ILLUSTRATING ANISOTROPIC HYSTERESIS.

Martensite of deformation obtained as a result of shock mechanical impact can occupy a considerable part of the material volume. It is known that the structure of deformation martensite can have a BCC lattice . However, Sidhom H., and Portier R. first discovered deformation martensite having an icosahedral structure (Frank- Kasper structure) . There are four types of tetrahedral close packed Frank – Kasper structures: FK-12, FK-14, FK-15 and FK-16 (figures correspond to the number of atoms on a polyhedron surface). Modeling the structures of martensite of deformation can help understanding the nature of structurization in bulk and film samples of Fe86Mn13C alloy under mechanical loading. In view of the above, an attempt has been made to model possible three-dimensional structures of martensite of deformation for bulk and film samples of Fe86Mn13C alloy using computer simulation. With three-dimensional graphics software, it is possible to model volume structures and solve the problem of finding the coordinates of already constructed points of models or objects.

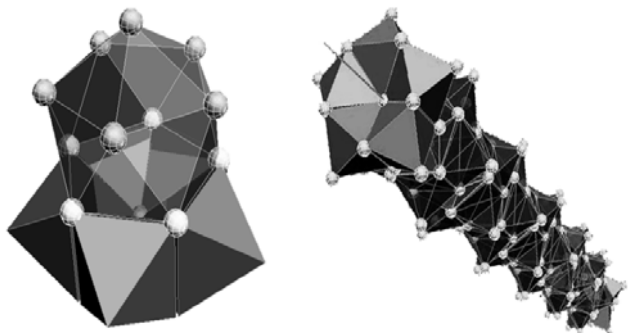


FIG. 10 THREE-DIMENSIONAL COMPUTER SIMULATION OF THE PROPAGATION STRING: PART OF THE STRING - A COMBINATION OF THE ICOSAHEDRON (FC 12) AND FIVE OCTAHEDRONS (ON THE LEFT), THE PROPAGATION STRING CONSISTING OF AN ICOSAHEDRON (FC 12) AND FIVE OCTAHEDRON (ON THE RIGHT)

The structure of one of the three-dimensional models is given in fig. 10: a string propagation. The three-dimensional model of string propagation is a combination of an icosahedron (FK-12) and five octahedrons forming a pentagonal "axis". In this manner, a model of formation of deformation martensite needles in Fe86Mn13C steel was constructed. The model was built based on the X-ray diffraction analysis data obtained for bulk Fe86Mn13C samples (see fig. 3, 8).

Structural modeling of martensite of deformation for thin film samples of Fe86Mn13C alloy was performed on the basis of electron diffraction pictures (fig.11).

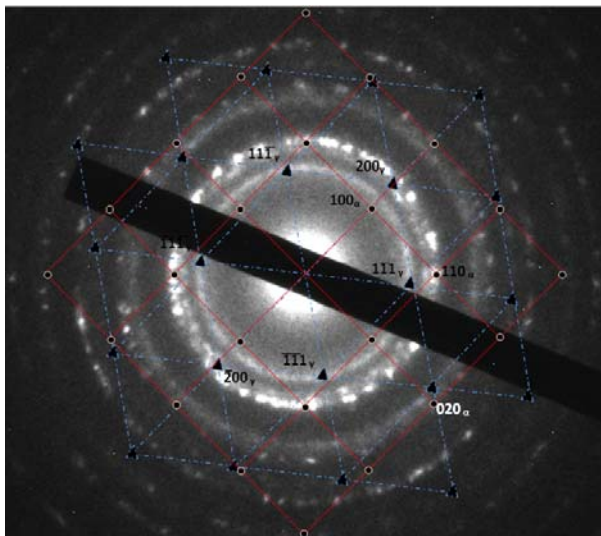


FIG. 11 A. ELECTRON MICRODIFFRACTION PICTURE OF THE FE86MN13C FILM

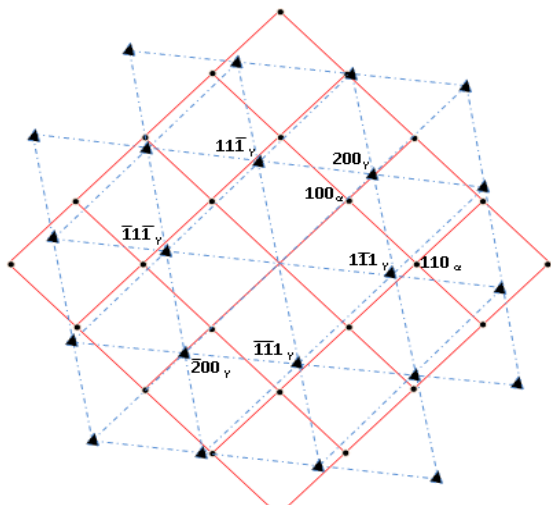


FIG. 11 B. SCHEME OF INTERPRETATION OF ELECTRON MICRODIFFRACTION (FIG. 11, A). THE SCHEME IS SIMILAR TO THE ONE PRESENTED BY YIFENG LIAO, FANLING MENG AND IAN BAKER.

Interpretation of the diffraction picture revealed the existence of coherently connected clusters of austenite having an FCC lattice and martensite having a BCC lattice with a doubled parameter compared to the α -Fe lattice. A similar diffraction picture was reported by Yifeng Liao, Fanling Meng and Ian Baker where formation of deformation martensite in bulk samples of high-manganic austenitic steel was studied.

In fig. 12, a rhombic icosahedron comprising six octahedral simplexes of a BCC-lattice presented is obtained by sectioning the cubic lattice by (110) typeplanes. Fig. 12 shows an elementary cell of the FCC-lattice that contains a rhombohedron consisting of an octahedron and two tetrahedrons sharing common sides. Fig. 12 illustrates the possibility of the acquisition of a BCC-lattice of martensite from the

FCC-lattice of austenite by small nuclear shifts. The edge of a fragment of the assembly representing an octahedron of the BCC-lattice can be combined with the edge of an octahedron of the FCC lattice as shown in fig. 12c. Here the octahedron of BCC-lattice is in the top part of the assembly. The arrows show possible movement of atoms of the FCC-lattice during formation of deformation martensite. Such movement is initiated by external mechanical influence. The model shown in fig. 12 suggests that the chemical bond can be switched and deformation martensite can be obtained as a product of mechanochemical reaction.

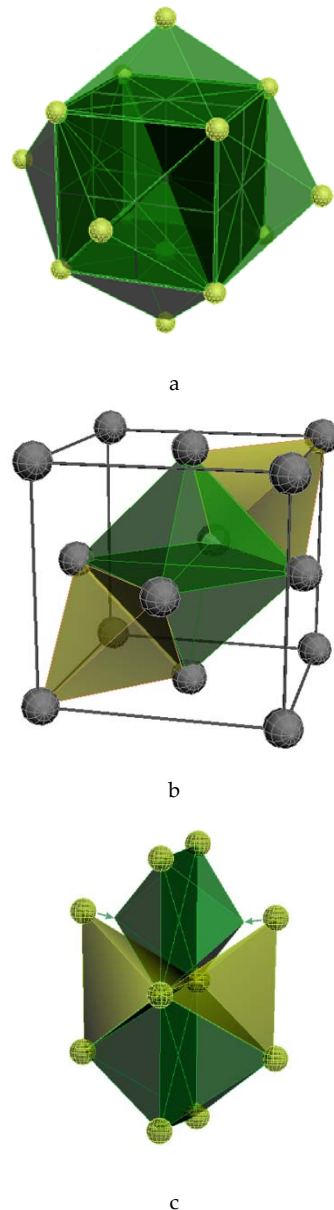


FIG. 12 COMPUTER SIMULATION OF 3D CLUSTERS, FOR A) BCC MARTENSITE, B) FCC AUSTENITE, C) THE SCHEME OF TRANSITION BETWEEN FCC AND BCC CLUSTERS, ARROWS SHOW THE POSITIONS OF THE ATOMS REPLACEMENT FCC \Rightarrow BCC.

The three-dimensional models of possible structural

transformation of austenite into deformation martensite can explain the anisotropy of the properties of both bulk and film samples of Fe86Mn13C alloy.

Conclusions

The non-uniform structure and magnetic properties of plastically deformed volume samples of Fe86Mn13C alloy with the highest values of impact strength have been investigated. The deformed alloy acquires magnetic viscosity which is visible as a discrepancy of hysteresis sites on the torque curves at various angles of rotation .

Structural analysis of Fe86Mn13C films by means of high-resolution electron microscopy, diffraction of electrons and 3-dimensional modeling confirms the equivalence of the bulk and film structures. The study of magnetic properties of the films after cryomachining reveals that the film magnetization of has pronounced anisotropy.

Electric properties of Fe86Mn13C alloy show that the alloy behaves as a semiconductor. This behavior is qualitatively consistent with the results of the spin polarized calculation of martensite of deformation.

Correlation of the crystal structure with the unique magnetic and electric properties of Fe86Mn13C alloy can characterize it as a material for spintronics.

ACKNOWLEDGMENT

This work was supported by grant number 278 of the Ministry of Education and Science of the Republic of Kazakhstan.

The authors are grateful to M.N.Volochaev and the laboratory "IRGETAS" East Kazakhstan Technical University.

REFERENCES

- Bulenkov NA, Tytik DL / The modular design of icosahedral metal clusters. Izvestiya (ser chem.), 2001, No 1, pp. 1.
- Hirsch P., Howie A., Nicholson R., Peschl J., Whelan M., Electron Microscopy of thin crystals. Transl. from English. - Springer-Verlag, 1968, 562.
- Kryannin I.R. Improving the quality of steel castings 110G13L, State M.: Scientific and technical publishing engineering literature, 1963, p.157.

Kveglis L.I., Abylkalykova R.B., Noskov F.M., Arhipkin V.G., Musikhin V.A., Cherepanov V.N., Niavro A.V./Local electron structure and magnetization in beta-Fe86Mn13C // Elsevier Superlattices and Microstructures, V46, 2009,p.116-120.

Kveglis L.I., Abylkalykova R.B., Semchenko V.V., Volochaev M.N / The variable thermoelectric Effect in magnetic viscosity Alloy Fe86Mn13C // VII International Conference on Mechanochemistry and Mechanical Alloying INCOME 2011, August 31-September 3, 2011, Herceg Novi.

Panichkin U.V., Abylkalykova R. B., Kveglis L.I., Semchenko V./The Sign-alternating Thermoelectric Effect in Magnetic Viscosity Alloy Fe86Mn13C// Scientific Israel-Tecnological Advantages" V.12, No 3, 2010, P. 30-35.

Pearson B. The Crystal chemistry and physics of metals and alloys (Wiley, New York, 1972; Mir, Moscow 1977). 418 p.

Sedov V.P. Antiferromagnetism gamma-iron. Invar problem. Moscow: Nauka, 1987. 287.J. S.I. Shablaev, R.V. Pisarev, Huge nonlinear absorption in NIO anti-ferromagnetic, FTT, 2003, V. 45, No 9, p 1660-1663.

Sidhom H., Portier R. / An icosaedral phase in annealed austenitic stainless steel//Philosophical Magazine Letters, 1989, V. 59, No 3, P. 131-139.

Stoner E. C., Wohlfarth E. P. A Mechanism of Magnetic Hysteresis in Heterogeneous Alloys // Philos. Trans. R. Soc. London, Ser. A.. — 1948. — V. 240. — No 826. — P. 599-642.

Temkin D. The rate of growth of the crystal needles in a supercooled melt/ Reports of the USSR, 1960, 132, 6, 1307-1310. Zangero. Phys.14, 200, (1962).

Vasilyev L.S. Structural phase transitions and critical phenomena with intense plastic deformation and fracture of metals and alloys. Abstract for the degree of Doctor of Physical and Mathematical Sciences. Izhevsk. 2010.

Yifeng Liao, Fanling Meng, Ian Baker / L12 precipitates within L21 ordered Fe-21.7Mn-14.5Al// Philosophical Magazine Vol. 91, Iss. 27, 2011.